New measurement of the ^{68}Zn(4_1^+) g factor combined with a reanalysis of previous data

K. Moschner,[1] K.-H. Speidel,[2] J. Leske,[3] C. Bauer,[3] C. Bernards,[1] L. Bettermann,[1] M. Honma,[4] T. Möller,[3] P. Maier-Komor,[5] and D. Mücher[1,5]

[1]*Institut für Kernphysik, Universität zu Köln, Zülpicher Strasse 77, D-50937 Köln, Germany*
[2]*Helmholtz-Institut für Strahlen- und Kernphysik, Universität Bonn, Nussallee 14-16, D-53115 Bonn, Germany*
[3]*Institut für Kernphysik, Technische Universität Darmstadt, D-64289 Darmstadt, Germany*
[4]*Center of Mathematical Sciences, University of Aizu, Tsuruga, Ikki-machi, Aizu-Wakamatsu, Fukushima 965-8580, Japan*
[5]*Physik Department, Technische Universität München, James-Franck-Strasse, D-85748 Garching, Germany*

(Received 21 April 2010; published 6 July 2010)

We have remeasured and have redetermined the g factor for the 4_1^+ state in ^{68}Zn following inconsistencies between earlier measurements and a recent result. We have reanalyzed several former measurements by applying an alternative analysis procedure, which allows for determining the precession effect separately for each gamma detector implying less uncertainties in the background subtraction for the relevant spectra. In addition, all measured g-factor and $B(E2)$ data for the first 2^+ and 4^+ states in all stable even-A Zn isotopes and the radioactive ^{62}Zn, are compared with new large-scale shell model calculations based on the most advanced effective interaction in the fpg-shell model space.

DOI: 10.1103/PhysRevC.82.014301 PACS number(s): 21.10.Ky, 21.60.Cs, 27.50.+e

I. INTRODUCTION

The even-A Zn isotopes are among those fp-shell nuclei, which, due to extensive experimental data, are eminently suitable for testing subtle predictions of nuclear properties by large-scale shell model (SM) calculations. In particular, for the lighter Zn nuclei with mass numbers $A = 62$, 64, and 66, $f_{7/2}$, $p_{3/2}$, $f_{5/2}$, and $p_{1/2}$ are the most relevant orbitals of a realistic model space, whereas for the heavier isotopes with $A = 68$ and 70, the intruder $g_{9/2}$ orbital becomes equally important for describing these nuclei.

The first results of a series of new measurements of g factors and lifetimes for the Zn nuclei, which employ the combined technique of Coulomb excitation in inverse kinematics with transient magnetic fields (TF) were reported in Ref. [1]. These experiments focused exclusively on the first 2^+ states. The g-factor data and the $B(E2)$ values derived from the newly determined lifetimes were generally more accurate than former literature values, exhibiting small but significant variations with neutron numbers that gave rise to a maximum g factor and a minimum $B(E2)$ value for ^{68}Zn at $N = 38$. These dependencies were fairly well reproduced by large-scale SM calculations based on ^{56}Ni as an inert core, a model space with $f_{5/2}$, $p_{3/2}$, $p_{1/2}$, and $g_{9/2}$ valence orbitals, and the effective interaction KB3G from Ref. [2] (see Ref. [1]). Specific deviations of the calculated values from the experimental data were attributed to the exclusion of the proton $f_{7/2}$ orbital from the model space, thereby signifying a breaking of the ^{56}Ni core. This assignment was actually confirmed by an alternative calculation based on a ^{48}Ca core with the explicit inclusion of the $f_{7/2}$ orbital for protons [1,3], which also improved the agreement with the experimental data.

Subsequent experiments on the isotopes ^{64}Zn, ^{66}Zn, and ^{68}Zn were carried out at higher beam energies for the respective Zn projectiles which, in addition, provided data on the 4_1^+ states. The explicit study of the 4_1^+ states was motivated by the inherently enhanced sensitivity to higher j orbitals compared to the 2_1^+ state, and specifically to the $g_{9/2}$ orbital of the model space in question [4–6].

In most measurements, NaI(Tl) scintillators were used because of their superior γ-detection efficiency, whereby the limited energy resolution of these detectors was generally sufficient to separate all relevant γ lines in the respective γ spectra. Only for ^{68}Zn was this condition not well fulfilled, therefore, requiring Ge detectors with significantly better energy resolution.

The data obtained for ^{64}Zn [4,5] and ^{66}Zn [6], showed positive and very similar g-factor values for the 4_1^+ states $g(4_1^+) = +0.53(16)$ and $+0.65(20)$, respectively, whereas, for ^{68}Zn, the g factor of the 4_1^+ state appeared to have a negative sign, the average value, being $g(4_1^+) = -0.37(17)$ [5]. The latter result would imply a very strong admixture of the neutron $g_{9/2}$ orbital [with its negative Schmidt value $g(\nu g_{9/2}) = -0.425$] in the nuclear wave function, which, however, could hardly be explained by SM calculations (see also Ref. [5]). This surprising result motivated a remeasurement by using highly efficient Ge Clover detectors [7]. The measured value $g(4_1^+) = +0.6(3)$ was in clear contradiction to the earlier results [4,5] and in good agreement with the data of the other Zn isotopes. Besides this discrepancy, all other g-factor data from this remeasurement, in particular, for the 2_1^+ and 2_2^+ states, were in excellent agreement with the results of Refs. [4,5]. In this context, it must be noted that all experimental 4_1^+ data generally suffer from large errors caused by the low excitation cross-sections and the relatively small slope values of the γ-angular correlations that are responsible for the low accuracy of the precession effects.

This unsatisfactory situation, which concerns the $g(4_1^+)$ data of ^{68}Zn motivated the present measurements with a set of more efficient Ge detectors and a critical reevaluation of all former results [4,5]. In the following, we report, in detail, on the new measurement and compare the present results with those from a reanalysis of the previous data, by applying an alternative procedure that exhibits substantially

lower sensitivity to uncertainties in background subtraction for the respective γ-ray spectra. It is shown that this new procedure has significant advantages over the conventional treatment when the signal-to-background ratio becomes small.

II. EXPERIMENTAL DETAILS AND MEASUREMENTS

In the present measurements, a beam of isotopically pure ^{68}Zn, extracted as ZnO^- ions from natural material in the ion source, was accelerated to an energy of 180 MeV at the Munich tandem accelerator with intensities of about 20 e nA on the target. The multilayered target consisted of 0.46 mg/cm^2 natural carbon, deposited on a 3.61 mg/cm^2 Gd layer, evaporated on a 1.6 mg/cm^2 Ta foil, and backed by a 4.2 mg/cm^2 Cu layer. In addition, thin ($\sim$0.005 mg/cm^2) layers of natural titanium were deposited between the carbon and the gadolinium, and also between the tantalum and the copper, to ensure good adherence among these layers. The target was cooled to the temperature of liquid nitrogen and was magnetized to saturation in an external field of 0.08 Tesla, which was alternated in the up and down directions with respect to the γ-ray detection plane every 200 s.

The ^{68}Zn projectiles were Coulomb excited in collisions with the carbon nuclei of the target in inverse kinematics, whereby the recoiling carbon ions were detected in a Canberra Si detector of 300 mm^2 area and a 100 μm depletion layer, located at 0° relative to the beam axis and subtending an angle of $\pm$39°. A 5 μm thick Ta foil was placed between target and detector to stop the beam ions, but permitted the carbon recoils to pass through to the detector. The Coulomb excited Zn nuclei traversed the magnetized Gd layer at a mean velocity of $\sim 6.3 v_0$ ($v_0 = e^2/\hbar$). The spins of the states of interest were aligned in the Coulomb excitation process and experienced precessions in the TF of the Gd layer. The nuclei were ultimately stopped in the hyperfine-interaction-free environment of the copper backing.

The deexcitation γ rays were measured in coincidence with the forward-scattered carbon ions. Four large-volume single-crystal Ge detectors were used for γ detection; their relative photopeak efficiencies between 70% and 130% and energy resolutions permitted a very clear separation of all the γ lines emitted. The relevant level scheme of ^{68}Zn is displayed in Fig. 1, and a typical γ-coincidence spectrum is shown in Fig. 2. An additional Ge detector with 37% relative efficiency was placed at 0° with respect to the beam axis. The purpose of this detector was to measure lifetimes of the excited states by the Doppler-shift-attenuation method and also to serve as a monitor on target stability.

Particle-γ-angular correlations $W(\Theta_\gamma)$ have been measured with one moving detector and the three remaining detectors at fixed angles for normalization, to determine the slopes $|S| = [1/W(\Theta_\gamma)][dW(\Theta_\gamma)/d\Theta_\gamma]$ in the rest frame of the γ-emitting nuclei for $\Theta_\gamma^{\rm lab} = \pm 65°$ and $\pm 115°$, at which the sensitivity to the spin precessions was nearly optimal for all γ transitions of interest. The spin precessions in the TF have been measured in the conventional way as a rotation of the angular correlations with respect to the direction of the external magnetic field [8].

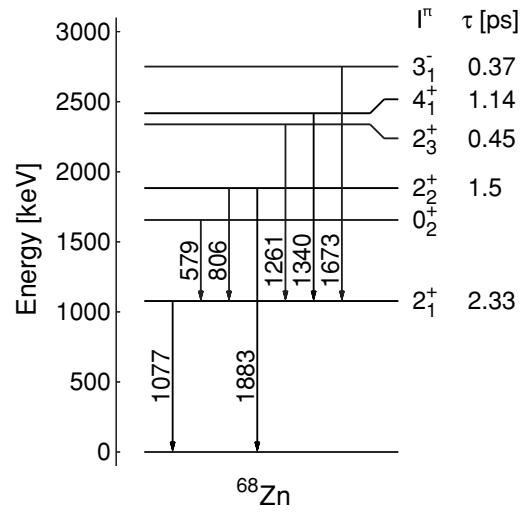

FIG. 1. Low-energy level scheme and relevant γ transitions in ^{68}Zn.

III. ANALYSIS AND RESULTS

The precession angles $\Phi^{\rm exp}$ were derived from the photopeak intensities N_i for up ($\uparrow$) and down ($\downarrow$) directions of the magnetic field via two different procedures:

(i) In the conventional way, denoted in the following as the *ratio procedure*, $\Phi^{\rm exp}$ is determined from intensity ratios R_{ij} of two pairs of detectors at backward (1,4) and forward (2,3) angles (placed symmetrically relative to the beam axis), which can be expressed as [4]

$$\Phi^{\rm exp} = \frac{1}{S}\frac{\sqrt{R_{ij}}-1}{\sqrt{R_{ij}}+1}, \tag{1}$$

where

$$R_{14} = \frac{N_1(\uparrow)/N_1(\downarrow)}{N_4(\uparrow)/N_4(\downarrow)} \quad \text{and} \quad R_{32} = \frac{N_3(\uparrow)/N_3(\downarrow)}{N_2(\uparrow)/N_2(\downarrow)}. \tag{2}$$

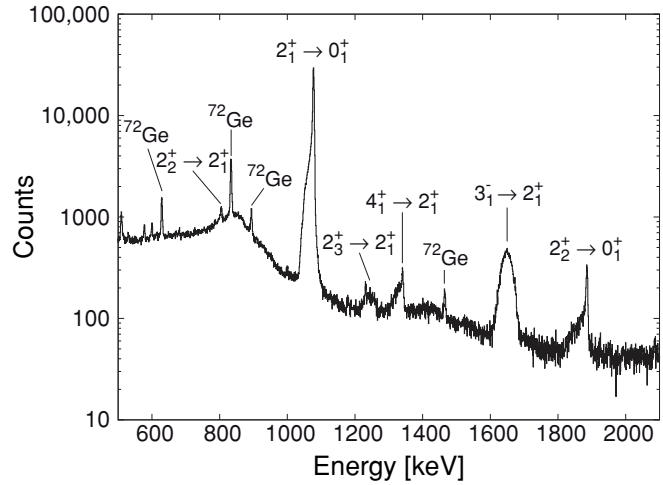

FIG. 2. Typical γ-coincidence spectrum of Coulomb-excited ^{68}Zn observed in a backward detector at $\Theta_\gamma^{\rm lab} = 115°$ gated by particles.

In these expressions, the photopeak intensities N_i and N_j $(i \neq j)$ in the coincidence spectrum of each detector have been corrected by subtracting a specific background under the peak for each field direction separately, as well as for random coincidence events. This procedure depends sensitively on the quality of fit to the shape of the background in the vicinity of the photopeak, a modality that is not free of uncertainties. It is especially challenging if the photopeak is sitting on a high background.

(ii) On these grounds, an alternative analysis procedure, denoted in the following as the *difference procedure*, has been adopted. It allows to determine, for each detector separately, an individual precession angle by using the following expression:

$$\Phi_i^{\exp} = \frac{1}{S_i} \frac{N_i^{\mathrm{tot}}(\uparrow) - N_i^{\mathrm{tot}}(\downarrow)}{N_i(\uparrow) + N_i(\downarrow)}, \tag{3}$$

where N_i^{tot} are the total uncorrected peak intensities, which give rise to the net precession effect in the difference between field up and down directions, since both the randoms and the backgrounds are quantitatively, consistently, and reliably subtracted. Specifically, they were free of the uncertainties in (i), bearing in mind that the field $\uparrow$ and $\downarrow$ spectra are accumulated over a time substantially longer than the field flipping time. Hence, beam-intensity variations during the accumulation time are averaged to zero for the two field directions as can also be seen in the difference spectra of the four detectors used (Fig. 3). The clear signature for this cancellation is the manifestation of a nearly zero-intensity level in the difference spectra everywhere in the measured pulse-height spectrum except in the regions of the lines that manifest a precession effect. Conversely, a nonrigorous cancellation would manifest itself in an offset of this level, which was not observed in any of the reanalyzed spectra of the present work. Moreover, even if such an offset were to be observed, data analysis according to the new procedure would merely require the subtraction of a simple well-determined and constant intensity fraction in the precession effect region of the difference spectra. Such a procedure would still be superior to the conventional analysis procedure with its inherent uncertainties as mentioned previously. Finally, it is noted that a careful inspection of this quasizero level in the difference spectra is indispensable, as precessions in the background regions cannot *a priori* be excluded. However, this procedure is performed under much cleaner conditions, and large effects are not expected.

Nevertheless, for the evaluation of the denominator in Eq. (3), one also needs to subtract random and background events. However, this is performed on the sum spectrum of the two field directions, which is less problematic, as first, the sum implies a zero precession effect, second, only one background needs to be subtracted, and third, counting statistics is higher and thereby more reliable than in (i). Altogether, with this procedure, one has good control over background subtraction uncertainties. Moreover, it also provides a built-in check, in that the individual precessions of the four detectors must be consistent within experimental errors.

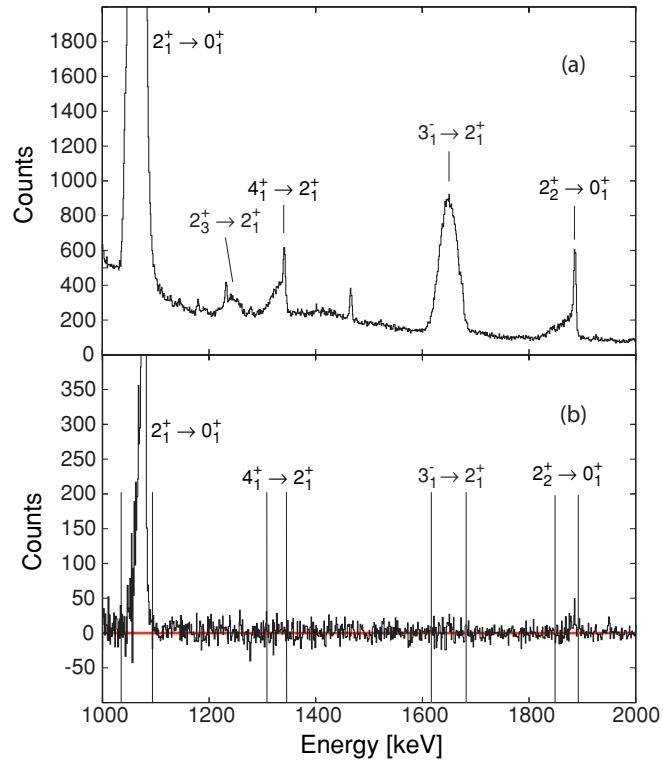

FIG. 3. (Color online) (a) Sum and (b) difference spectra of field up and down directions for a backward detector at $\Theta_\gamma^{\mathrm{lab}} = 115^\circ$. Windows drawn in (b) refer to the precession regions of the prominent γ lines displayed in (a).

As shown in Sec. IV, the two analysis procedures yield identical results if the peak (P) to the background (B) ratio P/B in the spectra is $\gtrsim 1$. This observation results from the reanalysis of present and other experimental data.

The g factor of the nuclear state in question is determined by the precession angle as given by [4]

$$\Phi^{\exp} = g \frac{\mu_N}{\hbar} \int_{t_{\mathrm{in}}}^{t_{\mathrm{out}}} B_{\mathrm{TF}}[v_{\mathrm{ion}}(t), Z_{\mathrm{ion}}] e^{-t/\tau}\, dt, \tag{4}$$

where B_{TF} is the effective TF, which acts on the nucleus during the time interval $(t_{\mathrm{out}} - t_{\mathrm{in}})$ that the ions spend in the Gd layer of the target; the exponential accounts for nuclear decay with lifetime τ while traversing the Gd layer.

The g factors were derived from the experimental precession angles by determining the effective transient field B_{TF} on the basis of the empirical linear parametrization (see, e.g., Ref. [8]),

$$B_{\mathrm{TF}}[v_{\mathrm{ion}}, Z_{\mathrm{ion}}] = G_{\mathrm{beam}} \cdot B_{\mathrm{lin}}, \tag{5}$$

with

$$B_{\mathrm{lin}} = a(\mathrm{Gd}) \cdot Z_{\mathrm{ion}} \cdot \frac{v_{\mathrm{ion}}}{v_0}, \tag{6}$$

where the strength parameter $a(\mathrm{Gd}) = 17(1)$ Tesla, and $G_{\mathrm{beam}} = 0.61(6)$ is the attenuation factor, which accounts for the reduced magnetization of the Gd layer induced by the

TABLE I. Summary of the slopes S of the measured angular correlations and the precession angles $\Phi^{\rm exp}$ derived by the *ratio* and the *difference procedures*. The $\Phi^{\rm lin}/g$ were calculated by using Eqs. (4)–(6) (see text).

I^π	τ (ps)[a]	$\lvert S\rvert$ (mrad^{-1})	$\Phi^{\rm exp}$ (mrad)		$\Phi^{\rm lin}/g$ (mrad)
			Ratio	*Difference*	
2_1^+	2.33(4)	2.13(9)	17.3(6)	17.5(6)	28.7(2.8)
4_1^+	1.14(6)	0.81(4)	0.7(11.5)	5.9(11.1)	26.1(2.6)
2_2^+	1.5(1)	1.8(4)	13(5)	15(5)	27.2(2.7)

[a]Reference [5].

energy loss of the Zn beam and which depends on the mean velocity of the excited Zn ions in the Gd layer (see Refs. [4,8]). It is noted that these data are consistent with many earlier values, which were obtained under very similar conditions.

The experimental results relevant to the precession analyses on the basis of the two above-mentioned approaches are summarized in Tables I and II. The slopes determined for the measured three angular correlations agree very well with previous data of independent measurements [5,7].

IV. DISCUSSION AND INTERPRETATION

Evidently, the g factors of the 2_1^+ and 2_2^+ states agree very well with previous data [4,5], and no significant difference is found in the two analysis procedures. This result is also expected, as the peak-to-background ratios of the two γ lines in question are $P/B \gtrsim 1$. In contrast, the g factor of the 4_1^+ state tends to be positive, in good agreement with the result of Ref. [7], but because of its large error, a small or even negative value cannot be completely excluded.

In view of the present new results and, in particular, with respect to the disputed 4_1^+ g factors, we have reanalyzed the precessions of all our former runs by applying the *difference procedure* as discussed before. The results from the two different approaches are summarized in Table III and are displayed in Fig. 4.

As seen from the data, there is very good agreement between the results from the two analysis procedures for the 2_1^+ and 2_2^+ states. However, for the 4_1^+ g factors, there is a clear trend towards positive values. The largest variation in this pattern is found for the data in which NaI scintillators exclusively were used, whereby the original negative value becomes zero or even positive. Due to the inferior energy resolution of these

TABLE II. Present g-factor results obtained from the *ratio* and the *difference procedures* in comparison to previous data [5,7].

I^π	$g(I)$		Ref. [5]	Ref. [7]
	Ratio	*Difference*		
2_1^+	+0.60(6)	+0.61(6)	+0.50(3)	+0.54(6)
4_1^+	+0.03(44)	+0.23(43)	−0.37(17)	+0.6(3)
2_2^+	+0.50(19)	+0.54(19)	+0.51(11)	+0.6(3)

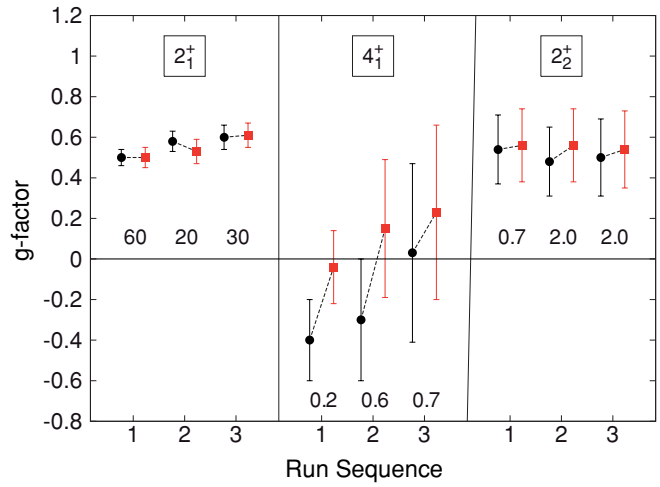

FIG. 4. (Color online) g-factor results of the 2_1^+, 2_2^+, and 4_1^+ states in ^{68}Zn derived by the *difference* (red color) and the *ratio* (black color) procedures for the present run 3 and two former runs 1 and 2 in 2004. The experimental P/B values are denoted below the data points (see text).

detectors, a large background fraction had to be subtracted under the $(4_1^+ \rightarrow 2_1^+)$ γ line, which introduces not only a large error, but also a high degree of uncertainty in the evaluation of the peak intensities. In this respect, the *difference procedure* for the evaluation of the precessions is far superior to the conventional method based on *intensity ratios*. It is noted that all such analyzed data are no longer in disagreement with the experimental result of Ref. [7] as shown in Fig. 5.

With the newly determined values, we finally obtain, for the weighted mean of the 4_1^+ g factor in ^{68}Zn,

$$g(4_1^+) = +0.14(13).$$

This value, in spite of its large error, is significantly smaller than the g factors of the 2_1^+ and 2_2^+ states in this nucleus, which indicates that neutrons indeed play an important role

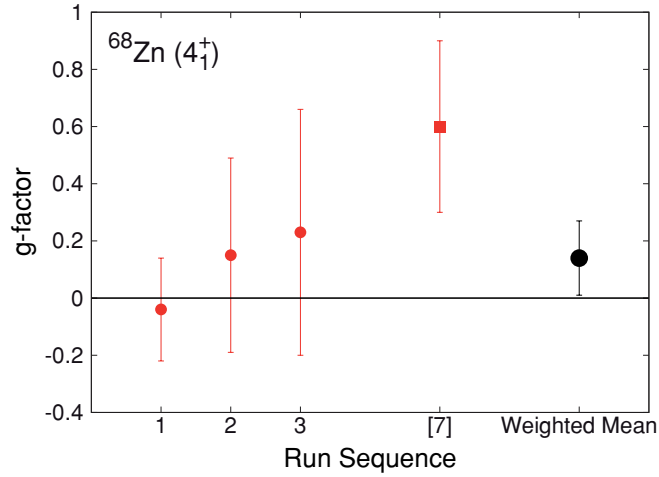

FIG. 5. (Color online) All three $g(4_1^+)$ values from the present run 3 and two former runs 1 and 2 in 2004 reanalyzed by the *difference procedure* in comparison to the result of Ref. [7] (square). Also shown is the weighted mean of all data (black color).

TABLE III. g-factor results of ^{68}Zn from the present and two former runs in 2004 analyzed by the two different procedures (see text).

Run	2_1^+		4_1^+		2_2^+	
	Ratio	*Difference*	*Ratio*	*Difference*	*Ratio*	*Difference*
1 2004	+0.51(4)	+0.50(5)	−0.4(2)	−0.04(18)	+0.54(17)	+0.56(18)
2 2004	+0.58(6)	+0.53(6)	−0.3(3)	+0.15(34)	+0.48(17)	+0.56(18)
3 2009	+0.60(6)	+0.61(6)	+0.03(44)	+0.23(43)	+0.50(19)	+0.54(19)

in the nuclear-wave function. It is clear that this implication needs to be studied in detail by SM calculations.

In view of the results for ^{68}Zn from the novel more reliable analysis procedure implemented in the present work, we have also reanalyzed the raw spectral data (where available) for the other Zn isotopes [4–6,9]. Also, in these cases, small changes of the values were found with the *difference procedure* in comparison to the previous values derived by the *ratio procedure*. All these data are summarized in Table IV together with the $B(E2)$ values of the $E2$ transitions deexciting the 2_1^+ and 4_1^+ states derived from the measured lifetimes of these states. In case of ^{68}Zn and ^{70}Zn, values for the 2_2^+ states have been included (see also, Ref. [9]).

In the following, we describe an attempt to account for these results within the framework of large-scale SM calculations based on a ^{56}Ni core with the recently discussed fpg-model space (with $f_{5/2}$, $p_{3/2}$, $p_{1/2}$, and $g_{9/2}$ active orbitals) and an appropriate effective interaction for describing fp-shell nuclei around the $N = Z = 50$ shell closures [10]. For the Zn isotopes, the inclusion of the $g_{9/2}$-intruder orbital is particularly important but as emphasized in Ref. [10], also, by breaking the ^{56}Ni core, the missing $f_{7/2}$ orbital might be essential for describing the lighter Zn nuclei. However, calculations in an enlarged model space with the explicit inclusion of the $f_{7/2}$ orbital is presently not feasible because of computer limitations.

For the calculations of the g factors, the magnetic-moment operator, which consists of spin $\vec{s}$ and orbital $\vec{l}$ contributions is given by

$$\vec{\mu} = g_s\vec{s} + g_l\vec{l}, \tag{7}$$

where g_s and g_l are the spin and the orbital g factors, respectively. For comparison with the experimental data, effective g_s and g_l values were used:

$$g_s^{\text{eff}} = 0.7g_s^{\text{free}} \quad \text{and} \quad g_l^{\text{eff}} = g_l^{\text{free}}. \tag{8}$$

The calculated values for the 2_1^+ and 4_1^+ states of several even-A Zn isotopes are displayed along with the experimental data in Fig. 6 and are summarized in Table IV (see also, Ref. [10]).

The agreement for the 2_1^+ and 2_2^+ values is striking. Even the small but pronounced rise of $g(2_1^+)$ towards ^{68}Zn with its maximum value at $N = 38$, is very well reproduced. Somewhat less good agreement for this dependence on the neutron number exists for the succeeding decrease to ^{70}Zn. Evidently, the effect of the $g_{9/2}$ neutrons with the respective negative Schmidt value is underestimated in the calculations.

In contrast, for the 4_1^+ g factors (despite their large experimental errors), this agreement between experiment and theory is not very good. Particularly, the prediction of the sharp decrease from $N = 32$ to $N = 36$ followed by the sudden rise to $N = 38$ and $N = 40$ is not seen in the experimental data. This irregular behavior of ^{66}Zn in the calculations is very likely caused by an incorrect mixing with the close-lying 4_2^+ state, which appears in the calculations only 182 keV above the 4_1^+ state with a g factor $g(4_2^+) = +0.464$. For ^{68}Zn with $N = 38$, the experimental g factor is indeed smaller than that of the 2_1^+ value, which calls for appreciable contributions from neutrons (see Fig. 6). Attempts to improve the present situation by changing the effective single-particle energies (especially the effective gap between the $f_{5/2}$ and $p_{1/2}$ orbitals) in the calculations eliminate the above-mentioned variations but are still insufficient to reproduce the overall dependence of the observed $g(4_1^+)$ values on the neutron number.

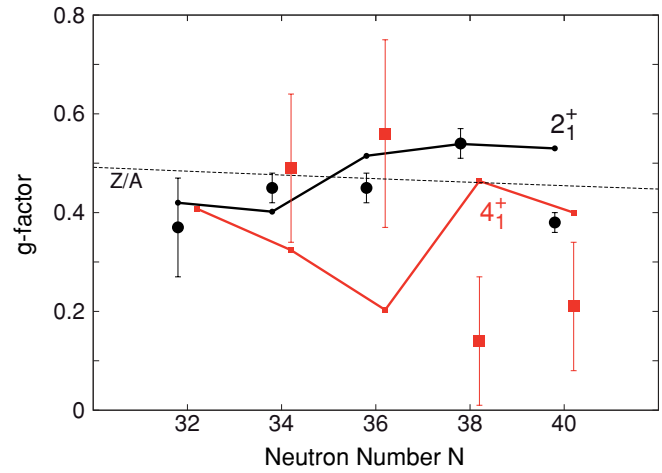

FIG. 6. (Color online) Experimental g factors of the 2_1^+ (circles) and 4_1^+ (squares) states as a function of the neutron number for several even-A Zn isotopes in comparison to SM calculations (small symbols). The lines drawn are to guide the eye.

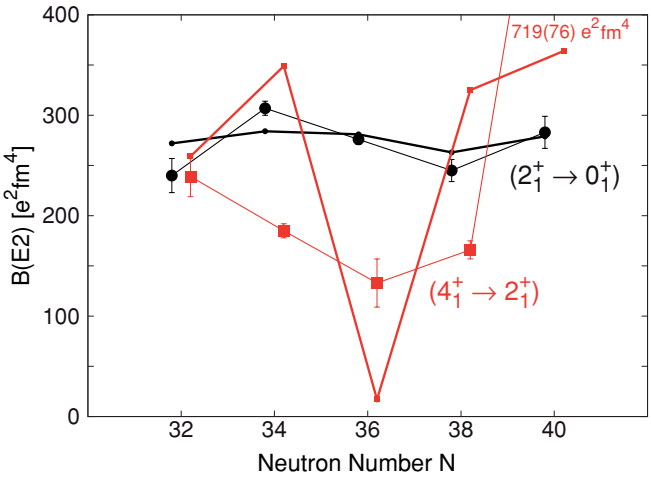

FIG. 7. (Color online) Experimental $B(E2)$ values for transitions from the 2_1^+ (circles) and 4_1^+ (squares) states as a function of the neutron number for several even-A Zn isotopes in comparison to SM calculations (small symbols). The lines drawn are to guide the eye.

For the reduced transition probabilities $B(E2)$, which generally describe the degree of collectivity of nuclei, the situation is very similar (see Fig. 7 and Table IV). The $(2_1^+ \rightarrow 0_1^+)$ and $(2_2^+ \rightarrow 0_1^+)$ values are rather well described by the calculations, which assume effective charges for protons and neutrons of $e_p = 1.5e$ and $e_n = 1.1e$, respectively. Even the small variations with the neutron number are very well reproduced. The quality of agreement in this case is comparable to that of the $g(2_1^+)$ and $g(2_2^+)$ values, which supports the assumptions inherent in the present calculations.

In contrast, the calculated $B(E2)$ values for the $(4_1^+ \rightarrow 2_1^+)$ transitions show large deviations from the experimental data by generally overestimating the collectivity. However, it is noted that the $B(E2)$ minimum at $N = 36$ is at least indicated by the calculations. This situation can be improved for ^{66}Zn and ^{68}Zn by additional modifications to those mentioned for the g-factor calculations (change in the relative gap between the $f_{5/2}$ and $g_{9/2}$ orbitals); however, the agreement in the g factors becomes worse.

To summarize, g factors have been remeasured for Coulomb excited states in ^{68}Zn. The new results, in particular, for the 4_1^+ state, were combined with reanalyzed data of several former measurements in which NaI scintillators and Ge detectors have been used for γ-ray detection. It was shown that the values of the 4_1^+ g factor depend sensitively on the reliability of background subtraction under the photopeak of the respective γ line. It was demonstrated that the *difference procedure* for field up and down photopeak intensities yields the most reliable precession results and the derived g factors accordingly. As a result of the data reanalysis undertaken in the present work, the g factor of the 4_1^+ state in ^{68}Zn no longer has a negative sign; within errors it agrees with the result of Ref. [7], but the average of all $g(4_1^+)$ values still tends to be smaller than that of

TABLE IV. Newly analyzed experimental g factors and already published $B(E2)$ values for 2_1^+, 2_2^+, and 4_1^+ states in several even-A Zn isotopes [1,4–6,9] compared to previous data and SM calculations.

Nucleus	I^π	$g(I)$			$B\left(E2, \begin{matrix} 2_1^+ \rightarrow 0_1^+ \\ 4_1^+ \rightarrow 2_1^+ \\ 2_2^+ \rightarrow 0_1 \end{matrix}\right)$ (e^2 fm^4)	
		Exp		SM	Exp	SM
		Present	Previous			
^{62}Zn	2_1^+	+0.37(10)	+0.37(10)[a]	+0.420	240(17)	272
$N = 32$	4_1^+	–	–	+0.408	239(20)	259
^{64}Zn	2_1^+	+0.45(3)	+0.45(3)[b]	+0.402	307(7)	284
$N = 34$	4_1^+	+0.49(15)	+0.53(16)[b]	+0.324	185(7)	349
^{66}Zn	2_1^+	+0.45(3)	+0.45(3)[c]	+0.515	276(5)	281
$N = 36$	4_1^+	+0.56(19)	+0.65(20)[c]	+0.203	133(24)	17
^{68}Zn	2_1^+	+0.54(3)	+0.50(3)[b]	+0.539	242(3)	263
$N = 38$	4_1^+	+0.14(13)	−0.37(17)[b]	+0.464	166(9)	325
	2_2^+	+0.55(11)	+0.51(11)[b]	+0.485	15(1)	12
^{70}Zn	2_1^+	+0.38(2)	+0.38(2)[d]	+0.530	283(16)	279
$N = 40$	4_1^+	+0.21(13)	+0.37(14)[d]	+0.400	719(76)	364
	2_2^+	+0.42(19)	+0.47(22)[d]	+0.541	10(2)	1

[a]Reference [1].
[b]Reference [5].
[c]Reference [6].
[d]Reference [9].

$g(2_1^+)$. The same behavior is also indicated by the reanalyzed ^{70}Zn data. This feature is a strong hint that, for these nuclei, $(g_{9/2})^2$-neutron configuration is a dominant component in the nuclear-wave function.

In addition, the experimental g factors and the $B(E2)$ values available for the 2_1^+, the 2_2^+, and the 4_1^+ states in several Zn isotopes have been compared with results from new large-scale SM calculations. While excellent agreement is found for the 2_1^+ and 2_2^+ data, there are substantial differences for the 4_1^+ results. To understand the existing deviations in this case will require further effort in the handling of a larger model space and refinements in the effective nucleon-nucleon interaction.

ACKNOWLEDGMENTS

The authors thank the operators of the Munich tandem accelerator laboratory. They are indebted to M. B. Goldberg (Soreq, Israel) and J. Jolie (Köln, Germany) for many valuable comments by their critical reading of the manuscript. The work was supported in part by the BMBF and the Deutsche Forschungsgemeinschaft.

[1] O. Kenn, K.-H. Speidel, R. Ernst, S. Schielke, S. Wagner, J. Gerber, P. Maier-Komor, and F. Nowacki, Phys. Rev. C **65**, 034308 (2002).

[2] A. Poves, J. Sánchez-Solano, E. Caurier, and F. Nowacki, Nucl. Phys. A **694**, 157 (2001).

[3] E. Caurier, F. Nowacki, and A. Poves, Eur. Phys. J. A **15**, 145 (2002).

[4] J. Leske, K.-H. Speidel, S. Schielke, O. Kenn, D. Hohn, J. Gerber, and P. Maier-Komor, Phys. Rev. C **71**, 034303 (2005).

[5] J. Leske, K.-H. Speidel, S. Schielke, J. Gerber, P. Maier-Komor, T. Engeland, and M. Hjorth-Jensen, Phys. Rev. C **72**, 044301 (2005).

[6] J. Leske, K.-H. Speidel, S. Schielke, J. Gerber, P. Maier-Komor, T. Engeland, and M. Hjorth-Jensen, Phys. Rev. C **73**, 064305 (2006).

[7] P. Boutachkov N. Benczer-Koller, G. J. Kumbartzki *et al.*, Phys. Rev. C **75**, 021302 (2007).

[8] K.-H. Speidel, O. Kenn, and F. Nowacki, Prog. Part. Nucl. Phys. **49**, 91 (2002).

[9] D. Mücher, G. Gürdal, K.-H. Speidel, G. J. Kumbartzki *et al.*, Phys. Rev. C **79**, 054310 (2009).

[10] M. Honma, T. Otsuka, T. Mizusaki, and M. Hjorth-Jensen, Phys. Rev. C **80**, 064323 (2009).